

Comparisons of binary black hole merger waveforms

John G. Baker,¹ Manuela Campanelli,^{2,3} Frans Pretorius,^{4,5,6} and Yosef Zlochower²

¹*Gravitational Astrophysics Laboratory, NASA Goddard Space Flight Center, 8800 Greenbelt Rd., Greenbelt, MD 20771, USA*

²*Center for Gravitational Wave Astronomy, Department of Physics and Astronomy,
The University of Texas at Brownsville, Brownsville, Texas 78520*

³*Center for Computational Relativity and Gravitation,
School of Mathematical Sciences, Rochester Institute of Technology,
78 Lomb Memorial Drive, Rochester, New York 14623*

⁴*Department of Physics, University of Alberta, Edmonton, AB T6G 2G7 Canada*

⁵*Canadian Institute for Advanced Research, Cosmology and Gravity Program*

⁶*Department of Physics, Princeton University, Princeton, NJ 08540*

(Dated: August 15, 2018)

This is a particularly exciting time for gravitational wave physics. Ground-based gravitational wave detectors are now operating at a sensitivity such that gravitational radiation may soon be directly detected, and recently several groups have independently made significant breakthroughs that have finally enabled numerical relativists to solve the Einstein field equations for coalescing black-hole binaries, a key source of gravitational radiation. The numerical relativity community is now in the position to begin providing simulated merger waveforms for use by the data analysis community, and it is therefore very important that we provide ways to validate the results produced by various numerical approaches. Here, we present a simple comparison of the waveforms produced by two very different, but equally successful approaches—the generalized harmonic gauge and the moving puncture methods. We compare waveforms of equal-mass black hole mergers with minimal or vanishing spins. The results show exceptional agreement for the final burst of radiation, with some differences attributable to small spins on the black holes in one case.

PACS numbers: EDIT 04.25.Dm, 04.30.Db, 04.70.Bw, 95.30.Sf, 97.60.Lf

The intense gravitational radiation produced by merging black-hole-binaries is expected to be among the strongest gravitational waves produced by astrophysical systems, and may even be detectable by the current generation of gravitational wave observatories, such as initial LIGO [1] (which is already taking data at its designed sensitivity). However, any detection with the current instruments is likely to be at a low signal-to-noise ratio, and therefore having accurate information about the predicted waveforms will increase the observers' ability to discern the signals from noise, effectively increasing the likelihood of an identifiable detection. For the more sensitive instruments to come, including advanced LIGO, and the space-based Laser Interferometric Space Antenna (LISA) observatory [2], better knowledge of the waveform predictions from General Relativity will increase the precision with which source parameters (i.e. the masses and spins of the components and the eccentricity of their orbit) can be identified from the waveform, and will make high-precision tests of General Relativity in the strong-field regime possible.

Recently several groups have independently made significant breakthroughs [3, 4, 5] in solving the Einstein field equations for coalescing black-hole binaries. Each of these groups were able to simulate the entire merger phase for various black-hole-binary configurations and accurately calculate the resulting waveforms. The novelty of the new techniques, however, leaves some room for questions of whether the results might be influenced by modeling errors that were not evident in the context of an individual research group's effort. In this paper we

compare the recently published results of three groups, which have each independently solved the problem of how to successfully evolve black-hole-binary systems through the last orbits, merger, and ringdown to extract the gravitational radiation. Each of these groups has performed simulations of systems of equal-mass black hole mergers [6, 7, 8, 9, 10] with the UTB and GSFC groups studying non-spinning irrotational binaries, while Pretorius applied a corotational binary model, implying a small spin $a/m = 0.08$ on each of the individual black holes. All simulations went through between 1.75 and 2.5 orbits before merger. Each of the groups has gone to some effort to demonstrate the quality of their waveforms, giving at least a rough estimate of the level of error in their simulations, but comparing the results gives us a more comprehensive understanding of the full range of modeling uncertainties.

If we look at waveform predictions as a modeling process, it is clear that there are several different classes of potential errors roughly associated with different steps in the modeling process. A first step is to pose initial data describing the configuration of the black holes at some point a few orbits before merger. In our comparisons, no attempt is made to fix the starting point of the simulations. Rather, we will look for agreement among the runs for the portion of the merger covered by all simulations. The runs shown here begin with a variety of initial data models. Pretorius uses the Cook-Pfeiffer [11, 12] technique to generate quasi-circular data using the conformal-thin-sandwich decomposition with excised horizon interiors. The GSFC and UTB groups

use the Brandt-Brügmann puncture approach [13] to generate the initial data (which, in turn, is based on the Bowen-York [14] ansatz for the extrinsic curvature). The GSFC and UTB approaches are distinguished by their respective choices of normalization and the methods used to determine the free initial data parameters. The GSFC group obtained values for the puncture positions and momenta from the Cook initial data sequence [15]. The UTB group, on the other hand, used the 3PN trajectories of quasi-circular binaries with an orbital period of $M\omega = 0.050$ and total mass $M_{ADM} = 1$ to determine the puncture positions, mass parameters, and momenta. The two choices of parameters turn out to be very similar; differing by less than 1% after re-normalizing to unit mass (the overall scaling is not important here because the waveforms will be rescaled by the final mass of the remnant).

The question here is how sensitive the waveform results are to variations in the initial data model. While it has not been straight forward for the groups individually to compare puncture models with Cook-Pfeiffer data, it is possible for each group to study initial data sensitivity within the class of initial data they are using. This has been addressed by the GSFC group by performing a range of simulations varying from the one presented here, to a four orbit run. Their simulations showed excellent agreement at roughly a 1% level beginning about $50M$ before the peak of merger radiation and onward. Prior to this late merger part of the waveforms, their waveforms showed rough agreement with variations that seemed to be associated with eccentric motion in the binaries that depended on the specifics of the initial data parameters for each run. Similar estimates of the intrinsic differences in Cook-Pfeiffer initial data sets were presented in [8] by evolving three different initial separations. Good agreement was also found near the peak of energy emission, though given that the corotation condition gave the initial black holes spins of 0.06, 0.08 (the simulation examined here) and 0.11, the agreement is not expected to be as close as the GSFC results.

All three approaches used conformally flat initial data. These data contain a short burst of spurious radiation that quickly leaves the system. The amplitude of this spurious signal decreases monotonically as the initial binary separation is increased and does not appear to alter the binaries waveform in a significant way after the pulse is radiated away.

The next, crucial stage in the modeling is to perform a numerical simulation of the merger dynamics. Pretorius' evolutions were performed using a generalized harmonic evolution scheme [16] with constraint damping [17]. Both the UTB and GSFC groups use the BSSN [18, 19, 20] system of equations in conjunction with a $1 + \log$ type lapse and Γ -driver shift conditions. The UTB method differs from the GSFC method in that the standard BSSN conformal exponent ϕ (which has an $O(\log r)$ singularity at the punctures) is replaced by the initially C^4 field $\chi = \exp(-4\phi)$, and by a different choice for the precise

form of the gauge conditions. The GSFC and Pretorius simulations took advantage of Adaptive Mesh Refinement, to allow a distant outer boundary without reducing resolution near the black holes, while the unigrid UTB simulations used a 'multiple transition' fisheye transformation [6] to push the physical boundaries to $216M_{ADM}$ (simulating FMR).

The final modeling step is to determine gauge invariant waveform information from the simulation data that represents the gravitational wave signal seen by distant observers. This is complicated by the fact that typical simulations require the radiation information be measured from the simulation data at relatively small distances from the sources in comparison to the far larger distances between earth-based observers and astrophysically realistic merging binaries. Again our groups have taken different approaches to this task. Working alone a group can quantify error levels by comparing waveforms extracted at different distances from the sources and by comparing the radiated energy and angular momentum with the mass and angular momentum differences between the remnant black hole mass and angular momentum and the ADM mass and angular momentum. In particular, the deviation between this mass difference and the radiated energy is a measure of the amplitude error in the waveform, while the deviation between this angular momentum difference and the radiated angular momentum is a measure of the phase error in the waveform as well as the amplitude error.

The UTB group used both the coordinate-based [21] and the quasi-Kinnersley [22, 23] tetrads to define ψ_4 (both extracted at $r = 30M$), and found no significant difference in the dominant ($\ell = 2, m = \pm 2$) modes for the two choices of tetrads. The coordinate-based tetrad is equivalent to the Kinnersley tetrad for Schwarzschild spacetimes, but the resulting Newman-Penrose ψ_4 contains contributions from the Kinnersley $\psi_0 - \psi_3$ for spacetimes with spin. The quasi-Kinnersley tetrad removes this type of mixing but leaves overall phase and amplitude ambiguities in ψ_4 . However, the good agreement between the radiated angular momentum and mass and the angular momentum and mass losses of the remnant black hole indicate that these amplitude and phase ambiguities are small for the ($\ell = 2, m = \pm 2$) modes. They verified the accuracy of the waveforms that they produced by evolving the binary with three resolutions and measuring the deviation in the waveforms between resolutions. They also confirmed that the radiated mass ($3.5 \pm 0.1\%$) and angular momentum ($27 \pm 1\%$) calculated from the waveform in their simulations matched the mass ($3.5 \pm 0.1\%$) and angular momentum ($26.9 \pm 0.3\%$) losses of the remnant horizon. The uncertainties in the radiated mass and angular momentum arise from extracting these quantities at finite distances and extrapolating to infinity. The uncertainty in the waveform due to finite resolution is quite small. After translating the waveforms so that the maximum amplitudes coincide and correcting for the phase differences at this maximum, they find

that the plunge part of the waveforms differ by $\sim 0.25\%$ between resolutions of $M/22.5$ and $M/27$, while the late-time ringdown part of the waveforms differ by $\sim 1.4\%$. The radiated energy and radiated angular momenta differ by 0.7% and 0.2% respectively.

The GSFC waveform simulations were carried out at three resolutions with finest-grid resolutions of $h_f \in \{3M/64, M/32, 3M/128\}$. At second-order convergence, the difference between these two higher resolution simulations provides a estimate for the error of the higher-resolution run. The peak wave amplitudes for these runs showed agreement to $\sim 0.5\%$, with differences of $\lesssim 1\%$ in the waveforms overall after shifting to align the peaks. The GSFC waveforms were extracted using a coordinate based tetrad, as in [21], but extractions were carried out on larger spheres $r/M \in \{20, 30, 40, 50\}$. Results from both higher-resolution runs including the three extraction radii with $r \geq 30M$ indicate consistent results for the radiative losses of energy ($3.44 \pm .01\%$) and angular momenta ($26.0 \pm .3\%$). In the comparisons we show waveforms from the $h_f = 3M/128$ run extracted at $r = 40M$, which strikes a good balance between $1/r$ effects too close in, and numerically induced dissipation as the waves propagate farther out.

In the generalized harmonic code waveforms were also extracted using a coordinate based tetrad at extraction radii from $r = 13M$ through $r = 51M$, as described in [8]. Convergence tests at an extraction radius of $r = 51M$ suggest a maximum amplitude error of 9% , a maximum bare phase error of 0.7 cycles, a maximum phase error after time translation and rotation of 0.06 cycles, ($4.3 \pm 0.4\%$) total energy radiated and ($33 \pm 2.1\%$) total angular momentum radiated.

We will compare the results of one run from each group. Table I summarizes the runs compared here. As stated, the runs agree in mass ratio and have vanishing or small spins. As we construct our comparison, we will initially ignore the small difference in spins, though we will return, as we consider the comparative results. The other physical parameters, total mass, merger-time, and merger-orientation are unrelated among our runs. Fortunately, each simulation result can be viewed as representing an equivalence classes of systems with different values for these parameters. Upon concretely simulating one member of the equivalence class, we can derive the others by suitable application of time-translation, rotation, and scaling operations. Our comparisons will focus directly on the strongly dominant spin-weighted spherical harmonic component of the radiation, the $(\ell = 2, m = 2)$ component (which is mirrored by the $(\ell = 2, m = -2)$ component). Following Refs. [7, 24] we will compare the simulations by rescaling masses by the final remnant black hole mass, applying a time-translation so that the time of peak waveform (polarization) amplitudes agree (labeled $t = 0$), and applying a rotation so that the waveform phases agree at $t = 0$. Note that a similar comparison method was introduced in Ref. [24].

In Fig. 1 we show the real part of the $(\ell = 2, m = 2)$

TABLE I: Model Parameters for the three runs. r_{ext} is the radius of the waveform extraction sphere, r_{bdry} is the location of the outer boundary, M_{ADM} is the total ADM mass of the system, J_{ADM} is the total ADM angular momentum, S is the initial horizon spins, τ is the initial orbital period, and ℓ is the initial proper distance between the horizons.

	Pretorius	GSFC	UTB
τ/M_{ADM}	153	127	126
ℓ/M_{ADM}	9.89	9.9	10.0
J_{ADM}/M_{ADM}^2	0.933	0.873	0.876
S/M_{ADM}^2	0.020	0	0
r_{ext}/M_{ADM}	50.6	40.2	30.0
r_{bdry}/M_{ADM}	∞	771	216

mode of ψ_4 for the three different simulations after normalizing the waveform by the final remnant mass, rescaling the t -axis by the final remnant mass, translating the waveforms so that the maximum amplitude is centered at $t = 0$, and multiplying by constant phase factors. As expected the UTB and GSFC waveforms are remarkably similar (i.e. they both start from essentially the same configuration), while Pretorius' waveform shows a higher frequency consistent with its larger spin. Note that the initial data pulse evident in the inset is smaller for Pretorius' waveform. This is mainly due to Pretorius' simulation starting from further separated binaries. The UTB and GSFC runs differ most strongly (but by less than 3% of the amplitude) at the peak of the waveform. Small differences in the UTB and GSFC waveform at the $O(1\%)$ level are expected because the initial data were only in agreement to that order. In addition the GSFC and UTB waveforms were extracted at different radii r_{ext} , and the extracted waveforms contain an $O(1/r_{\text{ext}})$ error. Note that the plunge behavior ($-25 < t/M_f < 25$) is in large part independent of differences in the starting configuration and initial spins (at least for small spins). This independence of the plunge waveform to small changes to the initial configuration is more pronounced in Fig. 2, which shows the instantaneous frequency of the $(\ell = 2, m = 2)$ mode of ψ_4 versus time. While Pretorius' simulation shows a generally consistent waveform, especially during the plunge, the frequency is slightly higher than that determined for the more similar GSFC and UTB waveforms during both the initial orbital inspiral part of the waveform and the late-time ringdown part of the waveform. We suspect that the differences may primarily be the effect of spin on the black holes in Pretorius' initial data, which tends to result in higher frequencies in merger and ringdown [25, 26, 27]. The relatively large oscillations observed in the UTB frequency profile at late times are due to boundary reflections, similar noise in the early part of the GSFC waveforms are caused by echos of early gauge dynamics off the AMR refinement interfaces.

From the above results we can make several important conclusions. First, the plunge part of the waveform is

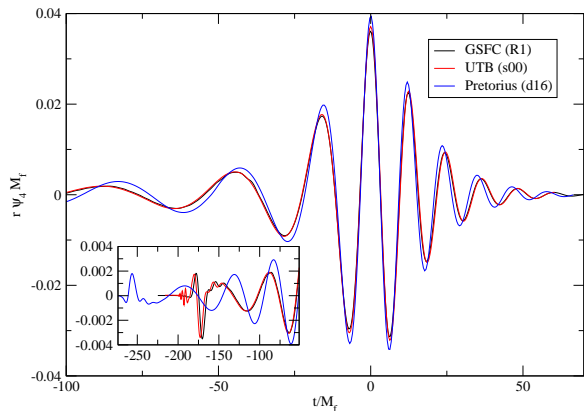


FIG. 1: The real part of the ($\ell = 2, m = 2$) mode of the gravitational radiation waveforms from three different research groups. The waveforms from the strictly non-spinning GSFC and UTB runs show excellent agreement after $t = -50M_f$, while Pretorius’ run rings-down at slightly higher frequency consistent with the corotating spins on the black holes. The inset shows the early part of the waveforms including the

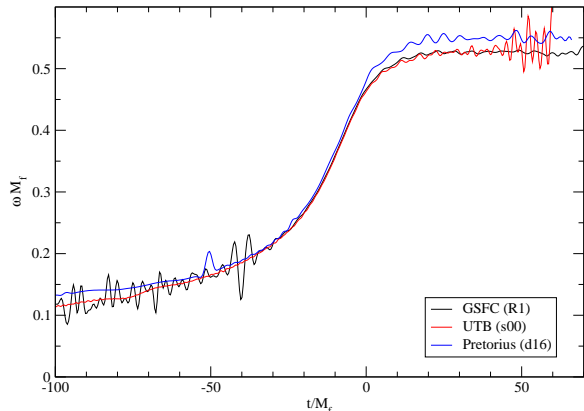


FIG. 2: Gravitational radiation polarization frequencies from three different research groups. The UTB and GSFC waveforms are very similar with the UTB result showing high frequency oscillation at late times due to boundary reflections. The consistently larger frequencies of Pretorius’ waveform are apparent.

a robust feature that varies little with either the binaries starting configuration or the component black hole spins (provided that the spins are small). Such universality of the late part of the waveforms was shown in [7] for a specific sequence of initial configurations with increasing separation. Our comparative results support the notion in a broader context. Second, the spurious radiation content of the initial data does not contaminate the

merger waveform significantly. Finally, the good agreement between these waveforms supports each individual groups claims of accuracy. On the other hand, our comparisons also seem to indicate that the GSFC and UTB waveforms agree more closely with each other than with Pretorius’ results which realize slightly higher frequencies. This difference is consistent with the small spins on the black holes in Pretorius’ simulations. Note however that the differences are in fact smaller than the conservative estimates of the errors of the latter simulation presented in [8]. Further comparisons of runs with more closely-matched astrophysical parameters and higher accuracy (both in terms of truncation error and controlling/understanding systematics) will be needed to verify that this is indeed the effect of astrophysical differences. Also, the comparisons presented here have been rather qualitative, and more rigorous, quantitative procedures will eventually be necessary—such a strategy was proposed in [28], though the emphasis there was on quantifying the accuracy and differences in waveforms with respect to the data analysis effort. It will be interesting to compare these waveforms, and those currently being produced by other groups, with this methodology. However, given that visually the three waveforms shown here are more similar than the sample waveforms used in [28] we can anticipate that the overlap of the waveforms in Fig. 1 will be greater than 0.95 for black hole binaries with masses greater than roughly 200 solar masses (see Fig.’s 2 and 8 in [28]).

The type of waveform comparisons illustrated in this paper will be facilitated by the NRwaves project [29], which will contain a repository of waveforms produced by all participating numerical relativity groups.

Acknowledgments

We thank Carlos Lousto and Pablo Laguna for careful reading of this text. M.C. and Y. Z. gratefully acknowledge the support of the NASA Center for Gravitational Wave Astronomy at University of Texas at Brownsville (NAG5-13396) and the NSF for financial support from grants PHY-0140326 and PHY-0354867. UTB simulations were performed on the 70-node “Funes” cluster at UTB, on the “Lonestar” supercomputer at TACC, and on the “Tungsten” supercomputer at NCSA. F.P.’s simulations were performed on the University of British Columbia’s “vnp4” cluster (supported by CFI and BCKDF), “WestGrid” machines (supported by CFI, ASRI and BCKDF), and “Lonestar”. F.P. gratefully acknowledges support from the CIAR, NSERC and Alberta Ingenuity.

[1] R. Vogt, in *Sixth Marcel Grossman Meeting on General Relativity (Proceedings, Kyoto, Japan, 1991)*, edited by

H. Sato and T. Nakamura (World Scientific, Singapore, 1992), pp. 244–266.

- [2] K. Danzmann and A. Rudiger, *Class. Quant. Grav.* **20**, S1 (2003).
- [3] F. Pretorius, *Phys. Rev. Lett.* **95**, 121101 (2005), gr-qc/0507014.
- [4] M. Campanelli, C. O. Lousto, P. Marronetti, and Y. Zlochower, *Phys. Rev. Lett.* **96**, 111101 (2006), gr-qc/0511048.
- [5] J. G. Baker, J. Centrella, D.-I. Choi, M. Koppitz, and J. van Meter, *Phys. Rev. Lett.* **96**, 111102 (2006), gr-qc/0511103.
- [6] M. Campanelli, C. O. Lousto, and Y. Zlochower, *Phys. Rev. D* **73**, 061501(R) (2006).
- [7] J. G. Baker, J. Centrella, D.-I. Choi, M. Koppitz, and J. van Meter, *Phys. Rev. D* **73**, 104002 (2006), gr-qc/0602026.
- [8] A. Buonanno, G. Cook, and F. Pretorius (2006), gr-qc/0610122.
- [9] M. A. Scheel et al. (2006), gr-qc/0607056.
- [10] B. Bruegmann et al. (2006), gr-qc/0610128.
- [11] M. Caudill, G. B. Cook, J. D. Grigsby, and H. P. Pfeiffer, *Phys. Rev. D* **74**, 064011 (2006), gr-qc/0605053.
- [12] H. P. Pfeiffer, L. E. Kidder, M. A. Scheel, and S. A. Teukolsky, *Comput. Phys. Commun.* **152**, 253 (2003), gr-qc/0202096.
- [13] S. Brandt and B. Brügmann, *Phys. Rev. Lett.* **78**, 3606 (1997), gr-qc/9703066.
- [14] J. M. Bowen and J. W. York, Jr., *Phys. Rev. D* **21**, 2047 (1980).
- [15] G. B. Cook, *Phys. Rev. D* **50**, 5025 (1994).
- [16] F. Pretorius, *Class.Quant.Grav.* **22**, 425 (2005), gr-qc/0407110.
- [17] C. Gundlach, J. Martin-Garcia, G. Calabrese, and I. Hinder, *Class.Quant.Grav.* **22**, 3767 (2005), gr-qc/0407110.
- [18] T. Nakamura, K. Oohara, and Y. Kojima, *Prog. Theor. Phys. Suppl.* **90**, 1 (1987).
- [19] M. Shibata and T. Nakamura, *Phys. Rev. D* **52**, 5428 (1995).
- [20] T. W. Baumgarte and S. L. Shapiro, *Phys. Rev. D* **59**, 024007 (1999), gr-qc/9810065.
- [21] J. G. Baker, M. Campanelli, and C. O. Lousto, *Phys. Rev. D* **65**, 044001 (2002), gr-qc/0104063.
- [22] C. Beetle, M. Bruni, L. M. Burko, and A. Nerozzi, *Phys. Rev. D* **72**, 024013 (2005), gr-qc/0407012.
- [23] M. Campanelli, B. Kelly, and C. O. Lousto, *Phys. Rev. D* **73**, 064005 (2006), gr-qc/0510122.
- [24] J. G. Baker, M. Campanelli, C. O. Lousto, and R. Takahashi, *Phys. Rev. D* **65**, 124012 (2002), astro-ph/0202469.
- [25] J. Baker, M. Campanelli, C. O. Lousto, and R. Takahashi (2003), astro-ph/0305287.
- [26] M. Campanelli, C. O. Lousto, and Y. Zlochower, *Phys. Rev. D* **74**, 041501(R) (2006), gr-qc/0604012.
- [27] M. Campanelli, C. O. Lousto, and Y. Zlochower, *Phys. Rev. D* **74**, 084023 (2006), astro-ph/0608275.
- [28] T. Baumgarte, P. Brady, J. Creighton, L. Lehner, F. Pretorius, and R. DeVoe (2006), gr-qc/0612100.
- [29] NRwaves home page: https://gravity.psu.edu/wiki_NRwaves.
-